Journal of Statistical Physics, Vol. 33, No. 2, 1983

Ising Model with Competing Interactions on a Cayley Tree

Sakari Inawashiro,[1,2,3] Colin J. Thompson,[2] and Goshi Honda[3]

Received March 31, 1983

An iterative scheme is developed for a renormalized effective nearest-neighbor coupling K_r and effective field per site X_r for spins in the rth shell of a Cayley tree with nearest neighbor J, and next nearest neighbor J', interactions between Ising spins on the lattice. In addition to the expected paramagnetic, ferromagnetic, and antiferromagnetic phases, we find an intermediate range of $J'/J < 0$ values where X_r and K_r iterate to a continuous or quasicontinuous attractor in the X–K plane. In this range the local magnetization is mainly chaotic with oscillatory glasslike behavior. Embedded in the chaos, however, are regions of periodic and commensurate phases.

KEY WORDS: Cayley tree; iteration; fixed points; cycles; attractors; chaos; spin glass; frequency locking; devil's staircase.

1. INTRODUCTION

The Ising model on a Cayley tree has been discussed by many authors; most recently by one of us[1,2] from the point of view of iteration. Local properties of the model with nearest-neighbor interactions only obtained from an iteration scheme from the outermost to innermost shell are in accord with the Bethe–Peierls approximation, and moreover in the limit of infinite coordination number one recovers the classical Curie–Weiss theory.[1] Also in this limit, the stable fixed point of the iterative shell-to-shell scheme for the quenched Gaussian random bond system is determined rigorously by the Sherrington–Kirkpatrick equations.[2]

[1] School of Physics, University of Melbourne, Parkville 3052, Australia.
[2] Department of Mathematics, University of Melbourne, Parkville 3052, Australia.
[3] Department of Applied Physics, Tohoku University, Sendai 980, Japan.

0022-4715/83/1100-0419$03.00/0 © 1983 Plenum Publishing Corporation

With nearest-neighbor interactions only there are no closed loops on the Cayley tree and hence no possibility of frustration effects. Not surprisingly one obtains in this case, for the nonrandom system,[1] only fixed points of the iteration scheme, corresponding to paramagnetic and ferromagnetic phases, with a bifurcation to an antiferromagnetic phase when the nearest-neighbor coupling constant changes sign. With competing next-nearest-neighbor interactions, frustration effects are possible and more exotic phases can be expected to appear. Indeed for the coordination number three model with nearest-neighbor interactions and competing next-nearest-neighbor interactions restricted to spins belonging to the same branch of the tree, Vannimenus[3] found, in addition to paramagnetic and ferromagnetic (fixed point) phases and a $++--$ periodic (four-cycle) antiferromagnetic phase, a modulated phase consisting of commensurate (periodic) and incommensurate (aperiodic) regions corresponding to the so-called "devil's staircase" found in the ANNNI[4] and other competing interaction models.[5] Similar periodic and chaotic trajectories have been found recently[6] in iterative renormalization group schemes which are exact on certain frustrated hierarchical lattices. It is natural to assume as was done in Ref. 6 that in these chaotic regions one is essentially observing a microscopic picture, or a random macroscopic picture, of glasslike behavior.

Independently of Vannimenus,[3] we also investigated the competing nearest- and next-nearest-neighbor Ising model on a Cayley tree[7] but unlike Vannimenus we considered the model with all interbranch interactions on the coordination number three lattice discussed earlier by Katsura and Takizawa.[8] The motivation for considering this model was based on the very high degree of frustration present and also because the model corresponds to the usual Bethe–Peierls approximation on the hexagonal lattice. Katsura and Takizawa[8] discussed the paramagnetic, ferromagnetic, and (period-four) antiferromagnetic phases in the spirit of the Bethe–Peierls approximation. Our aim was to study local properties of the model from the point of view of iteration with the expectation that some new phase might appear.

Our iteration scheme involves two quantities which can be interpreted physically; namely, an effective field X_r per site in the rth shell and an effective nearest-neighbor coupling constant K_r (incorporating the temperature) between spins in the rth and $(r+1)$th shell determined iteratively by summing successively over spins in the outermost (first) shell to the innermost shell, consisting of three spins surrounding the central spin σ_0 as shown in Fig. 1. The novel feature of our approach is that for most values of J and J' in a finite strip of $J'/J < 0$, where J' and J are, respectively, the next-nearest-neighbor and nearest-neighbor coupling constants, the X_r

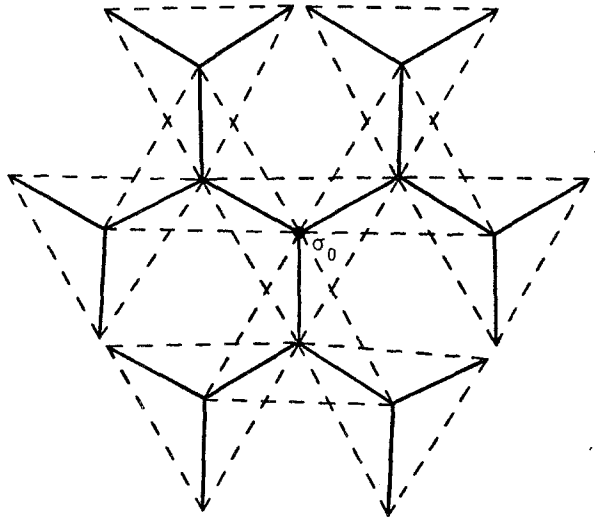

Fig. 1. Portion of a Cayley tree with coordination number three surrounding a central spin $\sigma_0 = \pm 1$. Full lines denote nearest-neighbor coupling and dotted lines denote next-nearest-neighbor coupling.

and K_r iterate to a continuous or quasicontinuous one-dimensional attractor in the X–K plane, giving rise to an oscillatory and chaotic local magnetization. Like Vannimenus, however, we find finite and small regions of periodic behavior or commensurate phases interspersed in this chaotic region. It is of course difficult to distinguish numerically between chaotic and long period sequences but we find to all intents and purposes that the new intermediate phase between paramagnetic and antiferromagnetic is predominantly chaotic.

In the following section we set up the model and derive the recurrence relations for the effective field X_r and the effective nearest-neighbor interaction K_r. Expressions for the local magnetization are given in Section 2 and these and the iteration scheme are examined numerically in Section 3. The main conclusions are discussed in the final section.

2. RECURRENCE RELATIONS

We consider a finite Cayley tree with coordination number three consisting of N shells surrounding a central spin σ_0, as shown in Fig. 1 for the case $N = 2$. We label the shells by an index r ranging from $r = 1$ for the outermost shell to $r = N$ for the innermost shell.

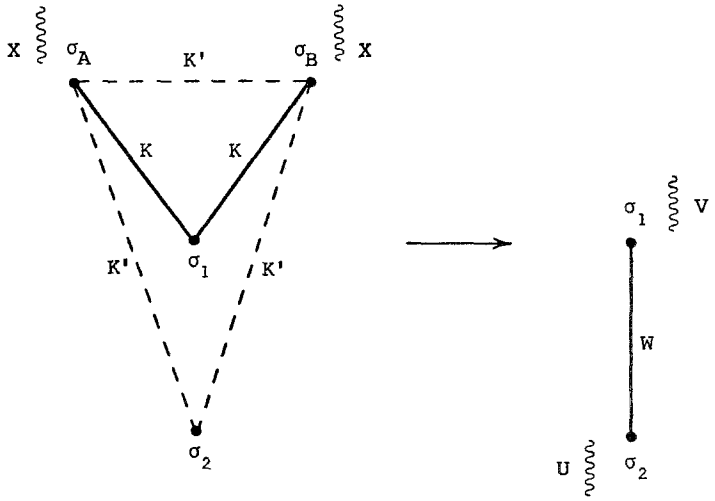

Fig. 2. Schematic illustration of selective summation of spins from the outermost to innermost shells.

In order to set up our iterative scheme we sum successively over spins in the outermost ($r = 1$) shell as shown schematically in Fig. 2. Simple but tedious algebra gives

$$\sum_{\sigma_A,\,\sigma_B=\pm 1} \exp\{K(\sigma_1\sigma_A + \sigma_1\sigma_B) + K'(\sigma_2\sigma_A + \sigma_2\sigma_B + \sigma_A\sigma_B) + X(\sigma_A + \sigma_B)\}$$

$$= C\exp(W\sigma_1\sigma_2 + U\sigma_2 + V\sigma_1) \tag{2.1}$$

where

$$U = U(X,K,K') = 4^{-1}\log[w(1,1)w(1,-1)/w(-1,1)w(-1,-1)] \tag{2.2}$$

$$V = V(X,K,K') = 4^{-1}\log[w(1,1)w(-1,1)/w(1,-1)w(-1,-1)] \tag{2.3}$$

$$W = W(X,K,K') = 4^{-1}\log[w(1,1)w(-1,-1)/w(1,-1)w(-1,1)] \tag{2.4}$$

$$w(\sigma,\sigma') = 2e^{K'}\cosh(2X + 2K'\sigma + 2K\sigma') + 2e^{-K'} \tag{2.5}$$

and

$$C = C(X,K,K') = [w(1,1)w(1,-1)w(-1,1)w(-1,-1)]^{1/4} \tag{2.6}$$

If we begin initially with an N-shell tree and incorporate the temperature by defining $K = J/kT$, $K' = J'/kT$ and $B = H/kT$ to be the nearest-

neighbor coupling, next-nearest-neighbor coupling and applied field per site, respectively, we obtain from (2.1) on summing over all spins in the first (or outermost) shell, a modified $(N-1)$-shell tree with effective outermost shell ($r=2$) field per site

$$X_2 = B + V(X_1, K_1, K') \tag{2.7}$$

and effective nearest-neighbor coupling between spins in the outermost ($r=2$) and next outermost shells ($r=3$) given by

$$K_2 = K + W(X_1, K_1, K') \tag{2.8}$$

The effective field per site in the original $r=3$ shell is given, from (2.1), by

$$X_3' = 2U(X_1, K_1, K') \tag{2.9}$$

the factor of 2 coming from the fact that two branches from the original $r=2$ shell meet at a single site in the $r=3$ shell. All other couplings and fields in the lattice remain unchanged, and for future convenience we have chosen

$$X_1 = B \quad \text{and} \quad K_1 = K \tag{2.10}$$

Repeating the above process it is not difficult to see that after summing over spins successively from the first to the $(r-1)$th shell, we induce an effective field X_r per site in what was the original rth shell, and an effective nearest-neighbor coupling K_r between spins in the rth and $(r+1)$th shells given recursively by

$$X_r = B + 2U(X_{r-2}, K_{r-2}, K') + V(X_{r-1}, K_{r-1}, K') \tag{2.11}$$

and

$$K_r = K + W(X_{r-1}, K_{r-1}, K') \tag{2.12}$$

where for convenience we have combined (2.7) and (2.9) and its iterates into one equation (2.11) by making use of the convention

$$X_0 = K_0 = 0 \tag{2.13}$$

[since from (2.2) and (2.6) $U(0,0,K') \equiv 0$].

Equations (2.11) and (2.12), with functions U, V, and W defined by equations (2.2)–(2.5) constitute our basic recursion relations and for an N-shell lattice, with initial conditions (2.10) and (2.13), may be iterated from $r=2$ to $r=N$. At the end point of this iteration we are left with a set of three spins, σ_N, σ_N', and σ_N'', surrounding the central spin σ_0 with effective four-spin Hamiltonian $\mathscr{H}_4^{(N+1)}$ given by

$$\begin{aligned} -\beta\mathscr{H}_4^{(N+1)} = {} & K_N\sigma_0(\sigma_N + \sigma_N' + \sigma_N'') + K'(\sigma_N\sigma_N' + \sigma_N'\sigma_N'' + \sigma_N''\sigma_N) \\ & + \left[B + 3U(X_N, K_N, K')\right]\sigma_0 + X_N(\sigma_N + \sigma_N' + \sigma_N'') \end{aligned} \tag{2.14}$$

the term $3U$ arising from the fact that three branches meet at the central spin.

Local properties involving expectation values of the innermost spins (σ_0, σ_N, σ'_N, and σ''_N) may be calculated directly from $\mathscr{H}_4^{(N+1)}$. For example, the expectation value of the central spin σ_0 for an N-shell tree which we define to be the *local magnetization* is given by

$$\langle \sigma_0 \rangle_N = \sum_{(\sigma_0, \sigma, \sigma', \sigma'')} \sigma_0 \exp(-\beta \mathscr{H}_4^{(N+1)}) \Big/ \sum_{(\sigma_0, \sigma, \sigma', \sigma'')} \exp(-\beta \mathscr{H}_4^{(N+1)}) \tag{2.15}$$

and is completely determined from X_N and K_N (as given in Appendix A).

The partition function for the complete lattice, from (2.1) and (2.6), is a product of factors $C(X_r, K_r, K')$. This and other bulk quantities for the model will not concern us here since, as is well known, the influence of boundary effects on bulk quantities results in a very peculiar type of phase transition.[9] These effects are eliminated by considering expectation values of quantities far removed from the surface such as $\langle \sigma_0 \rangle_N$. When $K' = 0$ in fact, $\langle \sigma_0 \rangle_N$ approaches the usual Bethe–Peierls expression as N approaches infinity.[1]

In the Appendix A we obtain expressions for shell magnetizations, that is, expectation values $\langle \sigma_r \rangle_N$ of spins σ_r in the rth shell. These can also be considered local quantities and an alternative definition of local magnetization could be

$$m = \lim_{n \to \infty} n^{-1} \sum_{k=1}^{n} m_k \tag{2.16}$$

where

$$m_k = \lim_{N \to \infty} \langle \sigma_{N-k} \rangle_N \tag{2.17}$$

is the limiting magnetization of spins in the kth shell outward from the central spin. Numerically at least, the shell magnetizations and $\langle \sigma_0 \rangle_N$ behave in a very similar fashion.

3. ITERATION OF THE RECURSION RELATION

Although in principle the recursion relations (2.11) and (2.12) provide us with an exact solution to the problem, one must in practice resort to numerical analysis of these relations. We have carried out such an analysis and the results are summarized in the phase diagram shown in Fig. 3.

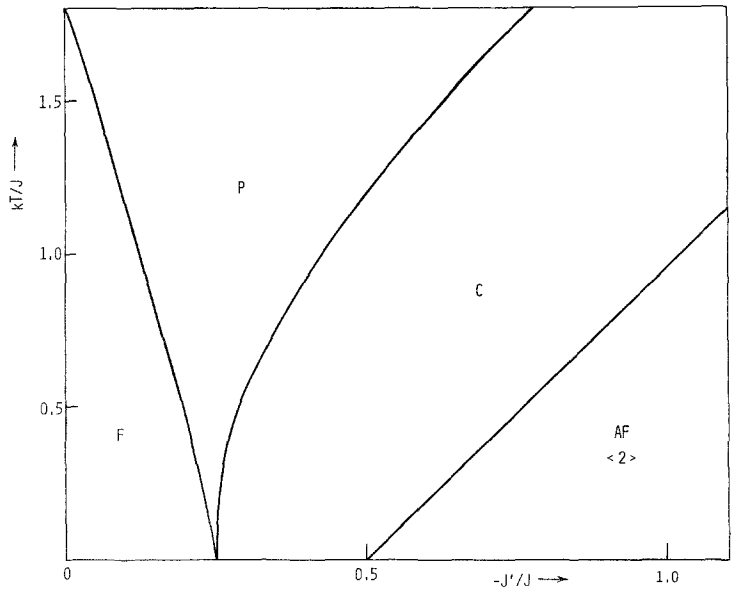

Fig. 3. Phase diagram showing ferromagnetic (F), paramagnetic (P), chaotic (C), and antiferromagnetic $+ + - -$ (A) phases.

3.1. The Phase Diagram

In order to obtain nontrivial results one must begin with $B \neq 0$ (at least for spins in the outermost shell) since otherwise the problem is essentially equivalent to the one-dimensional Ising model.[1] The limit $B \to 0$ should, therefore, only be taken after the thermodynamic limit. For numerical purposes, however, we must take some small finite B in the recursion relations. In all cases we chose $B = 10^{-5}$. Also in order to normalize the temperature scale we fixed $J/k = 1$ so that we have two independent variables, T and J'/J.

When J'/J is nonnegative we find, not surprisingly, that X_r and K_r approach a stable fixed point of (2.11) and (2.12). $\langle \sigma_0 \rangle_N$ then approaches a well-defined limit as $N \to \infty$ corresponding to a ferromagnetic state $\langle \sigma_0 \rangle > 0$ (at low temperatures) or a paramagnetic state $\langle \sigma_0 \rangle = 0$ (at high temperatures). The same states result when J' is negative and small in magnitude (relative to J). On the other hand, as shown in Fig. 3, when J' is negative and sufficiently large in magnitude, antiferromagnetic coupling between every second lattice site becomes important and X_r and K_r iterate to a four-cycle of points in the X–K plane yielding an antiferromagnetic $(+ + - -)$ state of the same form discussed previously by Katsura and

Takizawa.[8] This state, called a modulated $\langle 2 \rangle$ phase, was also obtained iteratively by Vannimenus.[3]

The interesting region occurs for intermediate negative values of J' where frustration takes hold and the system cannot decide whether it wants to be ferromagnetic or antiferromagnetic. The outcome is a predominantly chaotic phase in which iterates of (2.11) and (2.12) eventually fall on a continuous or quasicontinuous *attractor* in the X–K plane. An example is shown in Fig. 4 for parameter values $T = 0.2$, $J/k = 1.0$, $B = 10^{-5}$, and $J' = -0.3$.

When the local magnetization $\langle \sigma_0 \rangle_N$ is calculated in this intermediate region one typically obtains chaotic oscillatory behavior, as illustrated in Fig. 5 as a function of N. Moreover, we find numerically that the mean value

$$\lim_{B \to 0+} \lim_{n \to \infty} n^{-1} \sum_{k=1}^{n} \langle \sigma_0 \rangle_k = 0 \tag{3.1}$$

(or more correctly, the first limit is of order B for sufficiently small B).

In the case of periodic behavior, however, this is not necessarily the case. For example, in the case of period five (corresponding to the sequence $\langle 23 \rangle$ discussed below) the left-hand side of (3.1) is non-zero. All of the above results hold for the innermost to outermost iterative scheme and the corresponding shell magnetizations discussed in Appendix A.

The phase diagram, shown in Fig. 3, is qualitatively similar to Vannimenus' but differs in one very important respect, namely, in the ground state (along the $T = 0$ axis). Vannimenus found a triple or Lipshitz point at zero temperature corresponding to the meeting of the paramagnetic, ferromagnetic, and chaotic or modulated phases. In our model, however, the chaotic phase persists over a range of values of J'/J even at zero temperature. We attribute this important difference to the fact that our model is completely frustrated whereas Vannimenus' model is only frustrated along separate branches.

In the chaotic phase we found small regions with periodic orbits corresponding to commensurate phases. Although it is difficult, of course, to distinguish long period behavior from chaos, it seems that the behavior in the intermediate region is predominantly chaotic. Indeed, when one calculates the wave vector

$$q = \lim_{N \to \infty} \left[n(N)/2N \right] \tag{3.2}$$

defined by Vannimenus, where $n(N)$ is the number of times $\langle \sigma_0 \rangle_N$ changes sign, as a function of temperature (with fixed J'/J) we find that q has zero slope (corresponding to periodic behavior) only on very narrow T intervals.

For example when $J'/J = -0.55$ we found frequency locking with

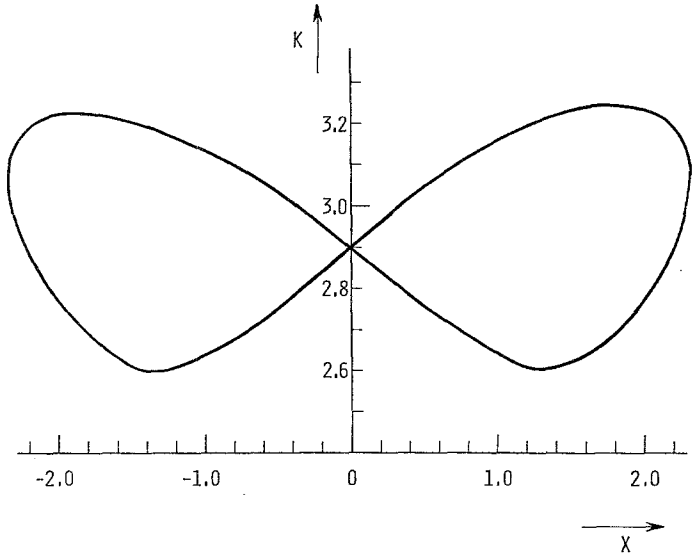

Fig. 4. An example of the attractor in the $X-K$ plane for parameter values $kT = 0.2$, $J = 1.0$, and $J' = 0.3$, obtained by iterating equations (2.11) and (2.12) on a computer for $r = 2, 3, \ldots, 1000$ and deleting the first 100 points.

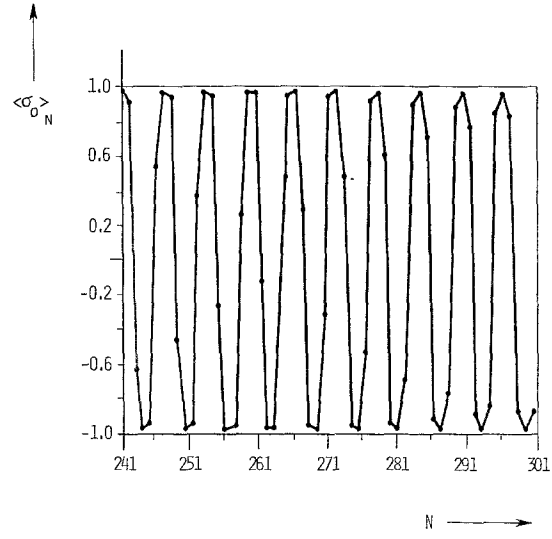

Fig. 5. Chaotic glasslike behavior of the local magnetization $\langle \sigma_0 \rangle_N$ as a function of N obtained from equation (2.15) for parameter values $kT = 0.4$, $J = 1.0$, and $J' = -0.35$.

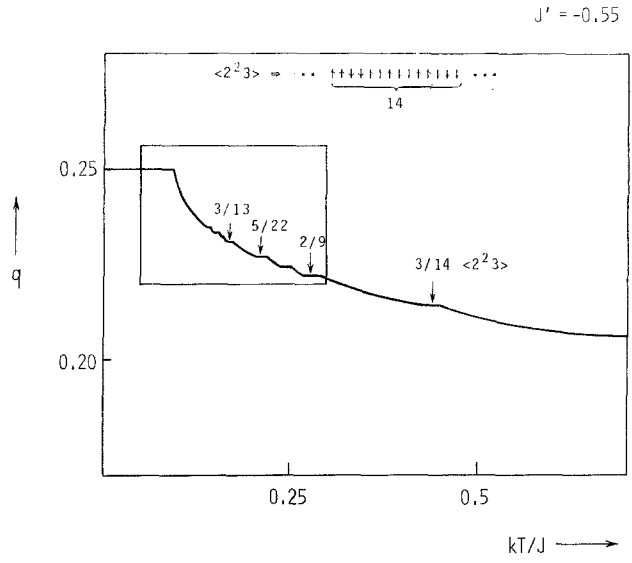

(a)

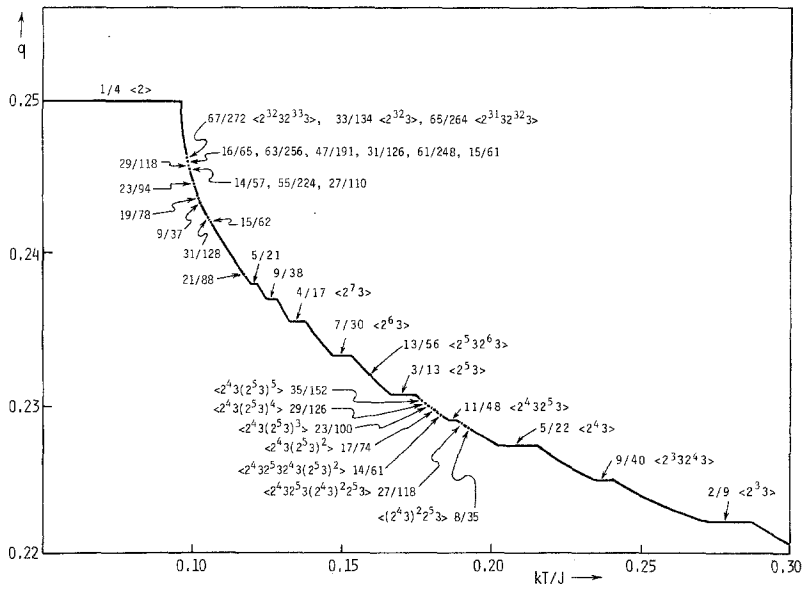

(b)

Fig. 6. The devil's staircase showing the wave vector q as a function of temperature T for J and J' fixed and $J'/J = -0.55$. Flat portions of the curve correspond to periodic behavior or frequency locking. (a) Overall temperature dependence of q; (b) A part of (a).

$q = 2/9$ for $0.270 < T < 0.284$ and with $q = 3/14$ for $0.426 < T < 0.438$ as shown in Fig. 6a.

One type of periodicity found for the local magnetization is characterized by a commensurate wave vector

$$q = l/2(2l + 1) \tag{3.3}$$

and corresponds to a cycle we denote by $\langle 2^{l-1}3\rangle$, which indicates a sequence of $l - 1$ pairs of local magnetizations pointing two "up" and two "down" followed by three local magnetizations all pointing up or down to maintain an overall "antiphase" character. An illustration for $\langle 2^2 3\rangle$, corresponding to $q = 3/14$, is shown in Fig. 6a.

Several examples of frequency locking for $J'/J = -0.55$ are seen as flat parts of the q–T curve shown on an enlarged scale in Fig. 6b. As can be seen from this figure, we found several types of hybridized sequences. For example, the sequence $\langle 2^{l-1}32^l 3\rangle$, characterized by the wave vector

$$q = \frac{2l + 1}{8(l + 1)} \tag{3.4}$$

was found in a temperature region between temperatures corresponding to cycles $\langle 2^l 3\rangle$ and $\langle 2^{l-1}3\rangle$. Also, as shown on Fig. 6b, we found cycles

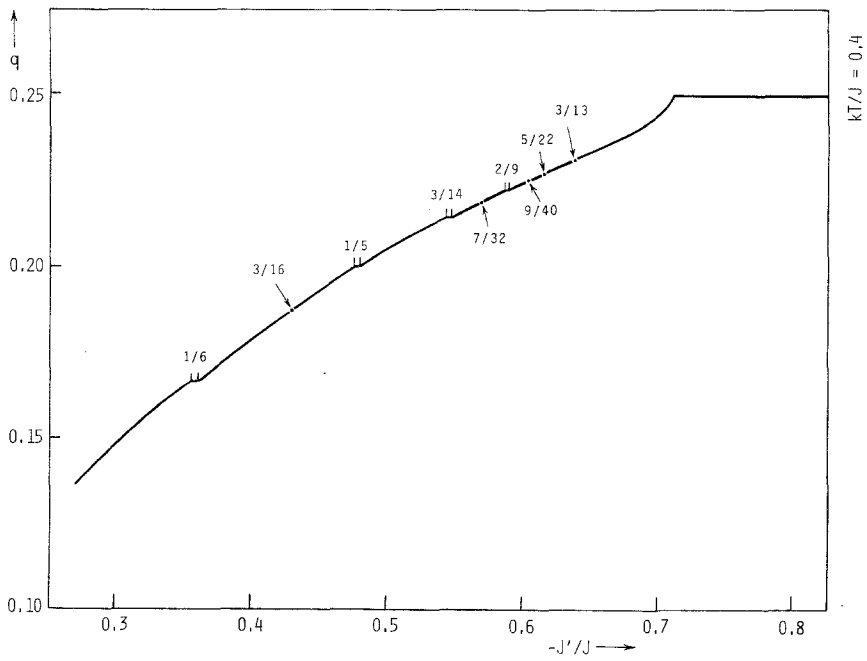

Fig. 7. The wave vector q as a function of $-J'/J$ for fixed temperature $kT = 0.4J$. Only several lockings for main commensurate phases are shown.

$\langle 2^4 3(2^5 3)^2\rangle$, $\langle 2^4 3(2^5 3)^3\rangle$, $\langle 2^4 3(2^5 3)^4\rangle$, and $\langle 2^4 3(2^5 3)^5\rangle$ in temperature regions between those of $\langle 2^5 3\rangle$ and $\langle 2^4 3 2^5 3\rangle$ and an extended sequence $\langle 2^4 3 2^5 3 2^4 3(2^5 3)^2\rangle$ between $\langle 2^4 3(2^5 3)^2\rangle$ and $\langle 2^4 3 2^5 3\rangle$. Similar types of sequences, and therefore locking of q, were found all over the chaotic region.

The largest period obtained numerically was of length 272 at $kT/J = 0.0979$ although undoubtedly there are longer period phases embedded in the chaos. In particular, the existence of long periods of the type $\langle 2^{l-1}3\rangle$ and $\langle 2^{l-1}32^{l}3\rangle$ close to $q = 1/4$ at low temperatures shown in Fig. 6b presumably arise from weak modifications of the fundamental $\langle 2\rangle$ antiphase.

The wave vector is also plotted as a function of $-J'/J$ for fixed temperature $kT = 0.4J$ in Fig. 7 where only several of the main cycles are shown.

It is tempting to conjecture on the basis of the observed proliferation of hybridized sequences of the form $\langle (2^{l_1}3)^{k_1}(2^{l_2}3)^{k_2}\cdots\rangle$ that the set of T regions where such phase locking occurs is dense on the line. (Or in other words between any two sequences of this form there is a third extended sequence of the same form.) In this case one might expect a general expression for q given by

$$q = (m+n)/(4m+5n) \tag{3.5}$$

in the interval $1/5 < q < 1/4$, for example, reflecting the so-called "period-adding phenomena" of nonlinear mappings.[11] Indeed, all values of q found so far in the interval $1/5 < q < 1/4$ can be expressed in the form (3.5) with (3.3) and (3.4) in particular obtained by taking $m = l-2$, $n = 2$ and $m = 2l-3$, $n = 4$ respectively. It may well be that the set of T values where locking does not occur has zero measure in which case we would have a complete rather than an apparent incomplete devil's staircase in Fig. 6a.

3.2. The Evolution and Nature of the Attractor

In our study of the chaotic region in the phase diagram we observed an interesting evolutionary phenomenon involving the attractor in the X–K plane, from its appearance at the boundary of the paramagnetic and chaotic phases to its eventual disappearance at the boundary of the chaotic and the antiferromagnetic phases.

For fixed temperature and decreasing negative J'/J, Figs. 8a–c show typical growth, evolution, and decay of the attractor. Firstly, when the paramagnetic fixed point becomes unstable, a small figure-eight attractor is born in its place (Fig. 8a) and grows to a larger figure-eight as $|J'|$ increases (Fig. 8b). The figure-eight then begins to droop (shown in Fig. 8c) and later develops gaps (a sure sign of ageing). The gappy-eight then develops two bottom pieces and a flat top, which further splits in two. The remaining

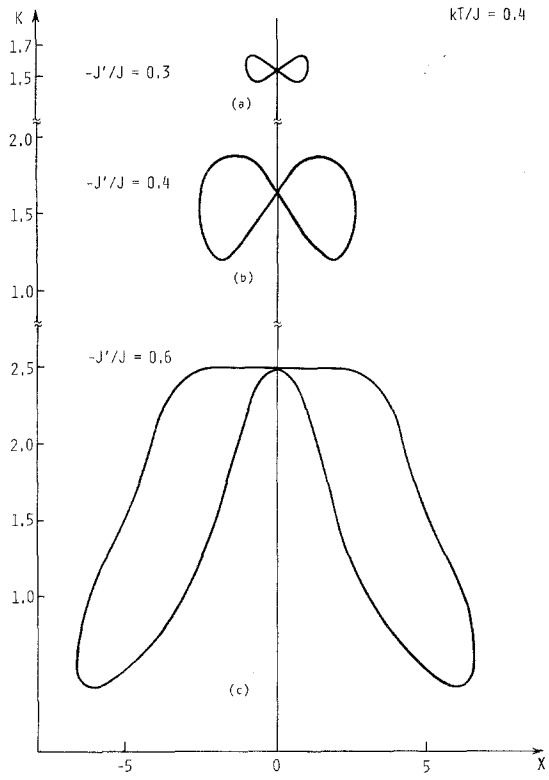

Fig. 8. Attractors showing typical growth, evolution and decay at $kT = 0.4J$. (a) $J'/J = -0.3$, (b) $J'/J = -0.4$, (c) $J'/J = -0.6$.

four pieces of the original figure-eight then contract until they become points of the antiferromagnetic four-cycle when the phase boundary between the chaotic and antiferromagnetic phases is crossed.

It is interesting that the birth, growth, and death of the attractor is essentially a continuous process but nevertheless punctuated here and there with a momentary collapse of the continuous or quasicontinuous attractor into a discrete set of points constituting a periodic cycle. We have also observed instances where the attractor takes on a Cantor setlike appearance although this is probably long cyclic behavior or even a very sparse quasicontinuous attractor.

In order to further investigate the nature of the attractor we have computed the Lyapunov exponent κ defined by

$$\kappa = \lim_{n\to\infty} n^{-1}\log|\lambda_{\max}(n)| \tag{3.6}$$

where $\lambda_{\max}(n)$ is the maximum eigenvalue of the product matrix $J_n J_{n-1} \cdots J_1 J_0$, where J_k is the Jacobian of a transformation (given in Appendix B),

which is equivalent to the transformation (2.11), (2.12), evaluated at the kth step of the iteration.

Recall that departure from differences in initial sets of data after n iterations is essentially given by $\exp(n\kappa)$ for large n, so that if the map is contracting, κ negative corresponds to cyclic behavior, whereas κ positive would usually correspond to a strange attractor. We find negative κ in the periodic intervals as expected, but typically κ is otherwise zero in the chaotic region corresponding to a continuous or quasicontinuous attractor. It is almost certain that our attractor is never strange.

4. CONCLUSIONS

In this paper we have studied the Ising model on a Cayley tree with competing nearest-neighbor ($J > 0$) and next-nearest-neighbor ($J' < 0$) interactions. By summing over successive shells from the outermost ($r = 1$) to innermost ($r = N$) shell we obtain recursion relations for effective fields X_r and *nn* interactions K_r which are rigorous, but which must in general be analyzed numerically.

For weak J', the dominant *nn* interaction J is responsible for ferromagnetic (or paramagnetic) behavior of the system, and a fixed point is reached in the recursion relations. On the other hand, when the *nnn* interaction J' is strong, antiferromagnetic coupling between every second lattice site becomes important and a four-cycle appears in the recursion relation corresponding to an antiferromagnetic $(++--)$ or $\langle 2 \rangle$ phase. For an intermediate range of the *nnn* interaction, however, frustration effects dominate and a new phase is obtained. In this new phase the recursion scheme exhibits a continuous or quasicontinuous attractor and this is reflected in chaotic behavior of the local magnetization. We also found narrow bands of periodic behavior in this intermediate region giving rise to a devil's staircase for the natural wave vector of the system.

As for periodic sequences of the local magnetization with commensurate wave vector q, the main sequence $\langle 2^{l-1}3 \rangle$, which is of the same form found in the ANNNI model,[4] was found numerically up to $l = 32$.

In addition to the main sequence we found new hybridized sequences of the form $\langle 2^{l-1}32^{l}3 \rangle$ and more complicated sequences $\langle 2^4 3(2^5 3)^m \rangle$ with $m = 2, 3, 4, 5$ as well as an extended sequence $\langle 2^4 32^5 32^4 3(2^5 3)^2 \rangle$. We believe that these types of sequences and possibly more generalized ones exist for other values of the parameters J'/J and T which may even form dense sets in the chaotic region.

In conclusion, it is interesting that as was also shown in Ref. 6 chaotic glasslike behavior can be obtained solely and rigorously from a model with competing nearest- and next-nearest-neighbor interactions without having to resort to the traditional, and somewhat artificial, introduction of

quenched bond disorder.[10] In view of the well-known connection between local properties on a Cayley tree and the Bethe–Peierls approximation on a corresponding translationally invariant lattice, it is tempting to speculate that similar phenomena, involving the full interplay between attractors and chaotic behavior, may be present on other frustrated regular lattices with competing interactions.

ACKNOWLEDGMENTS

We are grateful to the Australian Research Grants Scheme for their support and to T. Horiguchi for drawing our attention to the work of Vannimenus. S. I. would like to thank K. Kaneko for sending copies of his recent work. C. J. T. would also like to thank Derek Robinson and the Australian National University for their hospitality in January 1983 when part of this work was completed.

APPENDIX A. EXPECTATION VALUE OF AN ARBITRARY SPIN

In order to calculate expectation values of spins at arbitrary sites in the lattice it is convenient to start from the central spin and proceed outward to the outermost shell. For this purpose we need slightly more general expressions than those given in equations (2.1)–(2.6). Thus in place of (2.1) consider the four-spin system described by the Hamiltonian

$$-\beta\mathscr{H}_4 = K_A\sigma_1\sigma_A + K_B\sigma_1\sigma_B + K'(\sigma_2\sigma_A + \sigma_2\sigma_B + \sigma_A\sigma_B) + X_A\sigma_A + X_B\sigma_B \tag{A1}$$

We still have a formula analogous to (2.1), namely,

$$\sum_{\sigma_A,\,\sigma_B=\pm 1} \exp(-\beta\mathscr{H}_4) = C\exp(W\sigma_1\sigma_2 + U\sigma_2 + V\sigma_1) \tag{A2}$$

with U, V, W, and C given by (2.2), (2.3), (2.4), and (2.6), respectively, but now, in place of (2.5), we have

$$\begin{aligned} w(\sigma_1,\sigma_2) = {} & 2e^{K'}\cosh\left[X_A + X_B + 2K'\sigma_1 + (K_A + K_B)\sigma_2\right] \\ & + 2e^{-K'}\cosh\left[X_A - X_B + (K_A - K_B)\sigma_2\right] \end{aligned} \tag{A3}$$

Consider now the sequence of four-spin Hamiltonians

$$\begin{aligned} -\beta\mathscr{H}_4^{(r+1)} = {} & \tilde{K}_r\sigma_{r+2}\sigma_{r+1} + K_r\sigma_{r+1}(\sigma_r + \sigma_r') \\ & + \tilde{X}_r\sigma_{r+2} + X_r(\sigma_r + \sigma_r') + (B + 2U_r + \tilde{U}_r)\sigma_{r+1} \\ & + K'(\sigma_r\sigma_r' + \sigma_r'\sigma_{r+2} + \sigma_{r+2}\sigma_r) \end{aligned} \tag{A4}$$

for a system of four spins centered on σ_{r+1}, for $r = N, N-1, \ldots, 2, 1$, in

such a way that $\mathscr{H}_4^{(N+1)}$ represents the effective four-spin Hamiltonian for the central spin ($\sigma_0 \equiv \sigma_{N+1}$) of the original lattice, Eq. (2.14) so that X_r, K_r, and $U_r \equiv U(X_r, K_r, K')$ are obtained iteratively from (2.11) and (2.12). To begin a new iteration in reverse we choose

$$\tilde{X}_N = X_N, \quad \tilde{K}_N = K_N, \quad \text{and} \quad \tilde{U}_N = U_N \tag{A5}$$

In order to proceed outwards from the center we use (A2) in reverse with $\sigma_1 = \sigma_{r+1}$ and $\sigma_2 = \sigma_r$ to construct a six-spin Hamiltonian given via (A2) by

$$\begin{aligned} -\beta\mathscr{H}_6^{(r)} &= \tilde{K}_r\sigma_{r+2}\sigma_{r+1} + K_r\sigma_{r+1}\sigma_r + K_r\sigma_{r+1}\sigma_r' + K_{r-1}\sigma_r(\sigma_{r-1} + \sigma_{r-1}') + \tilde{X}_r\sigma_{r+2} \\ &\quad + (B + U_r + \tilde{U}_r)\sigma_{r+1} + X_r\sigma_r' + (B + 2U_{r-1})\sigma_r + X_{r-1}(\sigma_{r-1} + \sigma_{r-1}') \\ &\quad + K'(\sigma_r\sigma_r' + \sigma_r'\sigma_{r+2} + \sigma_{r+2}\sigma_r + \sigma_{r+1}\sigma_{r-1}' + \sigma_{r-1}'\sigma_{r-1} + \sigma_{r-1}\sigma_{r+1}) \end{aligned} \tag{A6}$$

We then use (A1), (A2), and (A3) to obtain

$$\sum_{\sigma_r', \sigma_{r+2} = \pm 1} \exp(-\beta\mathscr{H}_6^{(r)}) = \tilde{C}\exp(-\beta\mathscr{H}_4^{(r)}) \tag{A7}$$

where $-\beta\mathscr{H}_4^{(r)}$ is given by (A4) with r replaced by $r-1$, X_r and K_r are given by recurrence relations (2.11) and (2.12), and $\tilde{X}_r$ and $\tilde{K}_r$ are given by the outward recurrence relations

$$\tilde{X}_{r-1} = B + U_r + \tilde{U}_r + \tilde{V}_{r-1} \tag{A8}$$

and

$$\tilde{K}_{r-1} = K + \tilde{W}_{r-1} \tag{A9}$$

where

$$\tilde{U}_{r-1} = 4^{-1}\log[\tilde{w}_r(1,1)\tilde{w}_r(-1,1)/\tilde{w}_r(1,-1)\tilde{w}_r(-1,-1)] \tag{A10}$$

$$\tilde{V}_{r-1} = 4^{-1}\log[\tilde{w}_r(1,1)\tilde{w}_r(1,-1)/\tilde{w}_r(-1,1)\tilde{w}_r(-1,-1)] \tag{A11}$$

$$\tilde{W}_{r-1} = 4^{-1}\log[\tilde{w}_r(1,1)\tilde{w}_r(-1,-1)/\tilde{w}_r(1,-1)\tilde{w}_r(-1,1)] \tag{A12}$$

and

$$\begin{aligned} \tilde{w}_r(\sigma,\sigma') &= 2e^{K'}\cosh[X_r + \tilde{X}_r + 2K'\sigma + (K_r + \tilde{K}_r)\sigma'] \\ &\quad + 2e^{-K'}\cosh[X_r - \tilde{X}_r + (K_r - \tilde{K}_r)\sigma'] \end{aligned} \tag{A13}$$

The initial conditions are given by (A5) and the above relations hold for $r = N, N-1, \ldots$ to the outermost shell $r = 1$. The expectation value of a

typical spin in the rth shell is given by

$$\langle \sigma_r \rangle_N = \mathrm{Tr}\left[\sigma_r \exp(-\beta \mathscr{H}_4^{(r)}) \right] / \mathrm{Tr}\left[\exp(-\beta \mathscr{H}_4^{(r)}) \right] \equiv C_r / D_r \tag{A14}$$

where

$$\begin{aligned} D_r = {} & \exp(2K_{r-1} + \tilde{K}_{r-1}) \cosh(B_{r-1} + 2X_{r-1} + \tilde{X}_{r-1}) \\ & + \exp(-2K_{r-1} - \tilde{K}_{r-1}) \cosh(B_{r-1} - 2X_{r-1} - \tilde{X}_{r-1}) \\ & + \exp(-4K') \big[2 \exp(\tilde{K}_{r-1}) \cosh(B_{r-1} + \tilde{X}_{r-1}) \\ & \quad + 2 \exp(-\tilde{K}_{r-1}) \cosh(B_{r-1} - \tilde{X}_{r-1}) \\ & \quad + \exp(2K_{r-1} - \tilde{K}_{r-1}) \cosh(B_{r-1} + 2X_{r-1} - \tilde{X}_{r-1}) \\ & \quad + \exp(-2K_{r-1} + \tilde{K}_{r-1}) \cosh(B_{r-1} - 2X_{r-1} + \tilde{X}_{r-1}) \big] \end{aligned} \tag{A15}$$

$$B_{r-1} = B + 2U_{r-1} + \tilde{U}_{r-1} \tag{A16}$$

and C_r is obtained from (A15) by replacing the hyperbolic cosine functions with hyperbolic sine functions.

Note in particular, that the expectation value of the central spin (2.15) (in the present notation $\langle \sigma_{N+1} \rangle_N$) is given by (A14) with $r = N + 1$.

APPENDIX B. A TRANSFORMATION EQUIVALENT TO (2.11) AND (2.12)

The iterative equations (2.11) and (2.12) are easily rewritten in the more usual first order form

$$X_r = B + 2U_{r-1} + V(X_{r-1}, K_{r-1}, K') \tag{B1}$$

$$K_r = K + W(X_{r-1}, K_{r-1}, K') \tag{B2}$$

$$U_r = U(X_{r-1}, K_{r-1}, K') \tag{B3}$$

for three variables X_r, K_r, U_r. Introducing three new variables by

$$x_r = \exp(-2K_r)\left[\exp(2U_r) + \exp(2X_r) \right] / u \tag{B4}$$

$$y_r = \left\{ \exp\left[2(X_r + U_r) \right] - 1 \right\} / u \tag{B5}$$

$$z_r = \exp(-2K_r)\left[\exp(2U_r) - \exp(2X_r) \right] / u \tag{B6}$$

where

$$u = \exp\left[2(X_r + U_r) \right] + 1 \tag{B7}$$

we obtain an iterative scheme for these new variables similar to Vannimenus's,[3] namely,

$$x_{r+1} = \left[b^4\left(x_r^2 + z_r^2\right) + \left(1 + y_r^2\right) + 2(x_r + y_r z_r) \right] / a^2 D_r \tag{B8}$$

$$y_{r+1} = 2\left[b^4 y_r + x_r z_r + z_r + x_r y_r \right] / D_r \tag{B9}$$

$$z_{r+1} = -2\left[b^4 x_r z_r + y_r + z_r + x_r y_r \right] / a^2 D_r \tag{B10}$$

where

$$D_r = b^4\left(1 + y_r^2\right) + x_r^2 + z_r^2 + 2(x_r + y_r z_r) \tag{B11}$$

$$a = \exp(J/kT) \tag{B12}$$

$$b = \exp(J'/kT) \tag{B13}$$

Lyapunov exponents were calculated for the iterative scheme (B8), (B9), and (B10).

REFERENCES

1. C. J. Thompson, *J. Stat. Phys.* **27**:441 (1982).
2. C. J. Thompson, *J. Stat. Phys.* **27**:457 (1982).
3. J. Vannimenus, *Z. Phys. B* **43**:141 (1981).
4. M. E. Fisher, *Physica* **106A**:28 (1981).
5. P. Bak and J. von Boehm, *Phys. Rev. B* **21**:5297 (1980).
6. S. R. McKay, A. Nihat Berker, and S. Kirkpatrick, *Phys. Rev. Lett.* **48**:767 (1982).
7. S. Inawashiro and C. J. Thompson, *Phys. Lett. A*, to be published.
8. S. Katsura and M. Takizawa, *Prog. Theor. Phys.* **51**:82 (1974).
9. E. Müller-Hartmann and J. Zittartz, *Phys. Rev. Lett.* **33**:893 (1974).
10. S. F. Edwards and P. W. Anderson, *J. Phys. F.* **5**:965 (1975).
11. K. Kaneko, *Prog. Theor. Phys.* **68**:669 (1982).